RSC Advances

PAPER

View Article Online
View Journal | View Issue



Cite this: *RSC Adv.*, 2024, **14**, 15319

# Cellulose acetate microwell plates for high-throughput colorimetric assays†

Gabriela B. Gomez-Dopazo,[a] Renis J. Agosto Nieves,[a] Rolando L. Albarracín Rivera,[a] Shaneily M. Colon Morera,[a] Daniel Rivera Nazario,[b] Idalia Ramos,[b] Ivan J. Dmochowski,[c] Daeyeon Lee[d] and Vibha Bansal*[a]

Single use plasticware (SUP) in scientific, diagnostic, and academic laboratories makes a significant contribution to plastic waste generation worldwide. Polystyrene (PS) microwell plates form a part of this waste. These plates are the backbone of high throughput colorimetric measurements in academic, research, and healthcare settings for detection/quantification of wide-ranging analytes including proteins, carbohydrates, nucleic acids, and enzyme activity. Polystyrene (PS) microwell plates serve as a platform for holding samples and reagents, where mixing initiates chemical reaction(s), and the ensuing color changes are quantified using a microplate reader. However, these plates are rarely reused or recycled, contributing to the staggering amounts of plastic waste generated in scientific laboratories. Here, we are reporting the fabrication of cellulose acetate (CA) microwell plates as a greener alternative to non-biodegradable PS plates and we demonstrate their application in colorimetric assays. These easy to fabricate, lighter weight, customizable, and environmentally friendly plates were fabricated in 96- and 384-well formats and made water impermeable through chemical treatment. The plates were tested in three different colorimetric analyses: (i) bicinchoninic acid assay (BCA) for protein quantification; (ii) chymotrypsin (CT) activity assay; and (iii) alkaline phosphatase (AP) activity assay. Color intensities were quantified using a freely available smartphone application, Spotxel® Reader (Sicasys Software GmbH). To benchmark the performance of this platform, the same assays were performed in commercial PS plates too and quantified using a UV/Vis microplate reader. The two systems yielded comparable linear correlation coefficients, LOD and LOQ values, thereby validating the CA plate-cell phone based analytical method. The CA microwell plates, coupled with smart phone optical data capture, provide greener, accessible, and scalable tools for all laboratory settings and are particularly well-suited for resource- and infrastructure-limited environments.

Received 21st February 2024
Accepted 4th May 2024

DOI: 10.1039/d4ra01317d

rsc.li/rsc-advances



## 1 Introduction

According to data produced by UNESCO,[1] researchers account for approximately 0.1% of the global population but are contributing ~2% of plastic waste produced worldwide, most of which comes from single use plasticware (SUP). While scientific research is focussed on creating a better and healthier world for all, an average scientific researcher who performs experimental work, is inadvertently contributing 15 times more to plastic waste generation than the average person.[2] This is without taking into account the plastic waste generated by clinical and academic laboratories that also rely heavily on SUP. The driving force behind the extensive use of SUP in laboratories is the fear of contamination and the ease of use and throw practice. The most commonly used SUP include microwell plates, Petri plates, pipette tips, vials, tubes and bottles of various sizes. Dependence on SUP has become inherent to the point where most professors and researchers do not even evaluate the experimental design to determine if contamination is a real risk or problem in the scenario.

The action within the scientific community on this issue is surprisingly limited to a few laboratory initiatives and published reports.[2–6] Institutions that have tried to address this problem include University of Leeds which pledged to go single-use-plastic-free by 2023 (current status unknown) and University College London's pledge to follow suit, with a target date of 2024.[4] However, this drive can be successful only if viable alternatives are available to SUP in laboratories. The different

[a]*Department of Chemistry, University of Puerto Rico at Cayey, 205 Ave. Antonio R Barcelo, Cayey, PR-00736, USA. E-mail: vibha.bansal@upr.edu*

[b]*Department of Physics and Electronics, University of Puerto Rico at Humacao, CUH Station, 100 Road 908, Humacao, PR-00791, USA*

[c]*Department of Chemistry, University of Pennsylvania, 231S, 34th Street, Philadelphia, PA 19104-6323, USA*

[d]*Department of Chemical & Biomolecular Engineering, 220S, 33rd Street, Philadelphia, PA 19104-6323, USA*

† Electronic supplementary information (ESI) available. See DOI: https://doi.org/10.1039/d4ra01317d

routes away from the plastic waste generation include reusing the laboratory plasticware and using glassware wherever possible. The study being reported aims to provide a non-plastic alternative to the plastic microwell plates (also known as multiwell plates).

Multiwell plates have become an integral part of chemical/biochemical analyses as they enable simultaneous analyses of multiple samples, facilitating high-throughput screenings in didactic, research, and clinical settings.[7–11] Using microwell plates leads to substantial cost and time savings compared to approaches where samples are analyzed one at a time and typically require larger sample and reagent volumes. The analyte concentrations in these plates are measured using microplate optical readers that operate in UV/Visible regions. The design of these plates, made from polystyrene (PS), has evolved from 24-well format to 1536-well plates, increasing the number of samples that can be processed while facilitating analysis of much smaller sample volumes (2.39 mL to 12 μL). However these plastic plates are single use and non-biodegradable, thus contributing to the massive generation of non-recyclable waste in scientific laboratories.[6,12] In addition, despite the convenience of this research format, it requires availability of microplate readers that are expensive and inaccessible in non-laboratory field measurements or in laboratories with scarce resources.[13]

Cellulose-based analytical devices, also known as PADs and considered to be environmentally friendly and cheaper, have been in use for decades for several applications such as litmus paper, sensors, and point-of-care (POC) diagnostic devices, for example, for pregnancy, COVID-19, *etc.*[14–19] A new generation of PADs is under development as microfluidic devices: pieces of paper with micro zones and printed channels, which allow regulated sample flow and reagent mixing. Microfluidic devices enable sample analysis in sub-microliter volumes and testing for multiple analytes in the same sample.[16] Most reported devices of this type involve zone and channel formation through various kinds of printing techniques.[20] Paper microwell plates have also been fabricated where the wells are created by wax stamping[21] and photolithography[22] or wax printing on a piece of paper.[23] These cellulose-based devices are transforming the field of analytical methods, nevertheless they require sophisticated design (for specific applications) and fabrication infrastructure.[14,24,25] Also, given their non-standard geometries, most of the currently available technology (benchtop or smart phone based microplate readers) cannot be used for quantifying color intensities on such devices.[26]

In previous studies reported by our group, we chemically functionalized commercially available cellulose acetate (CA) discs and demonstrated their efficacy in fluorescence-based detection of analytes.[27,28] The growing interest in PADs, coupled to our previous experience in developing chemically derivatized CA discs for analyte detection, has inspired the work being reported in this manuscript. Amidst growing concerns over the staggering amount of plastic waste being generated in scientific laboratories worldwide,[6] and an immediate need to curb the use of single use plasticware,[3] here we report the fabrication of 96-well-format cellulose acetate (CA) plates as viable substitutes for plastic multiwell plates. The CA plates were designed on the format of traditional PS microwell plates and applied to colorimetric analyses. Our study demonstrates that these plates provide an easy-to-fabricate, customizable and biodegradable alternative to traditional PS microwell plates, without sacrificing performance.

# 2 Experimental

## 2.1 Materials

All reagents used were ACS grade and purchased from Millipore Sigma (USA). CA plates were fabricated using cellulose acetate (average $M_n \sim 50\,000$), calcium carbonate (≥99.0% purity, powder), acetone (≥99.5% (**https://www.sigmaaldrich.com/US/en/product/sigald/179124**) purity) and glycerol (≥99.5% purity). Hydrochloric acid (37%), diluted to 1 M, was used for removing calcium carbonate from the plates after the fabrication process.

Scotchgard Heavy Duty Water Shield (3M Science, Applied to Life™, USA) was used to spray coat the CA plates to increase hydrophobicity and water repellence. The microwell CA plates were examined through a JEOL JSM-IT100 scanning electron microscopy (SEM).

Spotxel® Reader: Plate Reader & Microarray Image Analysis, a free application available in the App Store and Google Play (**https://www.sicasys.de/spotxel-reader/**), was used for quantification of color intensities in colorimetric assays performed on CA microwell plates. This application can be downloaded and used on smartphones (both Apple and Android) as well as on Windows computers. The app works by analyzing the image of the microwell plate containing the reaction mixtures. The image can be taken in-app as well as imported to the app. The wells need to be aligned with the virtual plate template in-app and the app then reports color intensity values for each well. In this study, iPhone main cameras with a resolution of 12 MP (**https://www.apple.com/iphone/compare/?modelList=iphone-11,iphone-13,iphone-14-plus**), were used to capture images of the wells containing the reaction mixtures. This type of smartphone was chosen for convenience. The images were taken at an optical zoom of 1×.

Absorbances in colorimetric assays performed in Greiner 96 well PS plates (Millipore Sigma) were measured with an Epoch Microplate Spectrophotometer (Agilent Technologies).

## 2.2 Methods

### 2.2.1 Preparation of CA microwell plates

*2.2.1.1. 3D printing of the mold.* The microwell plate mold was designed in a Computer Aided Design (CAD) program (Autodesk Fusion). The design was then exported to CHITUBOX (a slicer program), which divides the 3D model into layers to be printed (Creality LD-002H resin printer). Each layer was 50 μm thick and had an exposure time of 1.8 seconds to radiation of 405 nm. Rapid Black Water-Washable 3D Printer Resin (Phrozen) was used for printing the mold.

*2.2.1.2 Fabrication of CA microwell plate.* Cellulose acetate (CA) solution containing CA (8% CA w/v in acetone) and glycerol

(6% v/v) was mixed with calcium carbonate (16% w/v)[29,30] resulting in a white dispersion. This mixture (approximately 40 mL) was poured into the microwell plate mold to fill it halfway and sprayed with a thin layer of deionized water. The mold containing the solution was then submerged into the water bath at 4 °C, and the lid pressed tightly into the bottom part of the mold to create the well indentations. Following this, the lid was removed, and another layer of CA dispersion poured (approximately 20 mL) on top of the previous layer, sprayed with deionized water, and submerged again in cold water bath with the lid pressing first lightly and then tightly into the bottom part of the mold. This process was repeated one more time to obtain a CA microwell plate with an even surface. The CA microwell plate was then placed in a r.t. (22–24 °C) water bath for 24 h and then annealed in a water bath at 85 °C for 1 h flipping the plate after 30 min.[31] $CaCO_3$ was then removed from the CA plate by placing the plate in 1 M HCl bath.[32] Finally, the plate was dried at r.t. (22–24 °C).

*2.2.1.3 Impermeabilization of the plate.* The CA microwell plates were sprayed with Scotchgard (commercially available impermeabilizing product) thrice with a drying time of 15 min after each application.

### 2.2.2 Characterization of CA microwell plates

*2.2.2.1 Scanning electron microscopy.* The CA microwell plate was imaged using SEM at the different stages of the fabrication process including post-fabrication, post-heat treatment, post-HCl bath and post-impermeabilization using a JEOL JSM-IT100 SEM microscope. The secondary electron detector (SED) was set to 5.0 kV for the analysis and a magnification of 60× was used.

*2.2.2.2 Impermeability characterization.* For testing the impermeability of the plate post treatment with Scotchgard, a drop of 10 μL of water was added to the plate. The time of absorption was then recorded. Additionally, the resistance of coating to different solvents, routinely used in colorimetric methods, was studied by adding 10 μL of solvents to different wells in the microplate. The solvents studied were 0.1 M NaOH and 0.1 M HCl. The wells were then imaged using SEM. The same wells were then subjected to water drop absorption experiments to verify if the treatment with any of these solvents had affected the impermeability of the plate.

**2.2.3 Colorimetric assays.** The application of the CA microwell plates for colorimetric estimations was demonstrated by using these to perform three different colorimetric assays in PS microwell plates as well as CA microwell plates.

*2.2.3.1 Bicinchoninic acid (BCA) assay.* Protein concentration was measured using the BCA method developed by Smith *et al.*[33] BCA Protein Assay kit from Sigma (**https://www.sigmaaldrich.com/US/en/product/mm/71285m**) was used for the purpose. Working BCA reagent was prepared by mixing BCA solution with 4% cupric sulphate solution in a ratio of 50 : 1 (v/v). A 1.0 mg $mL^{-1}$ solution of Bovine Serum Albumin (BSA) was used to prepare protein standard solutions in the concentration range of 6.67–33.33 mg $mL^{-1}$ using deionized water as diluent. To perform the assays, the working BCA reagent and protein solutions of different concentrations were mixed in a ratio of 8 : 1 (v/v) in 96-well plate, and the plate allowed to incubate at 37 °C for 30 min. The plate was then allowed to cool to room temperature, and quantification of the purple color resulting from reaction between protein and BCA reagent performed by measuring: (i) absorbance at 562 nm using a microplate reader in case of assay performed in 96-well PS plate; and (ii) color intensity using the Spotxel® Reader application on smartphone in case of assays performed in 96-wells CA plate. All measured absorbance/color intensity values were corrected for background signal by subtracting the absorbance/color intensity of the blank sample, containing only deionized water and working BCA reagent, from those of BSA (protein) containing reaction mixtures.

*2.2.3.2 Alkaline phosphatase (AP) assay.* The activity of AP was determined by monitoring AP catalyzed hydrolysis of a colorless substrate, *p*-nitrophenyl phosphate (PNPP), resulting in formation of *p*-nitrophenol (PNP), yellow in color.[34] PNPP solution (3.2 mM) was prepared in 0.025 M glycine/NaOH buffer (pH 9.6) containing 8.6 mM $MgCl_2$. AP dilutions were prepared in the range of 2–12 μg mL−1 in glycine/NaOH buffer (0.025 M; pH 9.6) containing 1 mM $MgCl_2$, 0.1 mM ZnCl2, and 10% glycerol. AP solutions of different concentrations were mixed with substrate (PNPP) in a ratio of 1 : 1 (v/v) in 96-well plate. The AP catalyzed hydrolysis of PNPP was measured immediately as: (i) absorbance at 405 nm using a microplate reader in case of assay performed in 96-well PS plate; and (ii) yellow color intensity using a the Spotxel® Reader application on smartphone in case of assays performed in 96-wells CA plate. All measured absorbance/color intensity values for enzyme activity were corrected for background signal by subtracting the absorbance/color intensity of the blank sample, containing only enzyme diluent buffer and PNPP, from those of enzyme containing reaction mixtures.

*2.2.3.3 Chymotrypsin (CT) assay.* CT activity was determined by monitoring CT catalyzed hydrolysis of colorless *N*-succinyl-Ala-Ala-Pro-Phe-*p*-nitroanilide (SAAPPpNA), resulting in the formation of *p*-nitroaniline (PNA).[35] Five different dilutions of CT (0.01–0.07 μM) and a 0.25 mM solution of substrate (SAAPPpNA) were prepared in Tris HCl buffer (0.1 M) containing $CaCl_2$. The enzyme and substrate were mixed in the 96-well plate in a 1 : 1 (v/v) ratio. The reaction was allowed to proceed at r.t. (22 °C) for 5 min and the hydrolysis of substrate leading to formation of PNA measured as: (i) absorbance at 410 nm using a microplate reader in case of assay performed in 96-well PS plate; and (ii) yellow color intensity using a the Spotxel® Reader application on smartphone in case of assays performed in 96-wells CA plate. All measured absorbance/color intensity values for enzyme activity were corrected for background signal by subtracting the absorbance/color intensity of the blank sample, containing only buffer and substrate, from those of enzyme containing reaction mixtures.

Attempts at reading the PS plates using a camera and the Spotxel® Reader did not yield good results because of the reflection of the color against the transparent background of the plates. The PS plates were thus read using a microplate reader. Results obtained for each of the three assays in CA plates using Spotxel® Reader were compared to the same assays performed in the traditional system that uses PS plates and microplate

reader. All measurements were performed in triplicate and the assays were repeated at least three separate times. Standard analyte activity (absorbance or color intensity *versus* analyte concentration) plots were prepared, and linear regression performed to obtain value of the slope. This data was further used to calculate Limit of Detection (LOD) and Limit of Quantification (LOQ) for each assay in both systems. LOD describes the smallest concentration of the analyte that can be detected by means of a given analytical procedure; while LOQ describes the smallest concentration of the analyte that can be quantified/measured with statistical significance by means of a given analytical procedure. LOD was calculated using the formula: $3\sigma$/slope and LOQ was calculated as $10\sigma$/slope.

# 3 Results and discussion

Colorimetric methods are prevalent in biochemical analyses and have wide-ranging applications that include protein quantification, enzyme activity determination, carbohydrate, nucleic acid, and metal ion detection.[34,36,37] Routinely, these methods are performed in microwell plates made of PS. In this study, we report the development of CA microwell plates as ecofriendly and user-friendly alternatives to the traditional PS plates, coupled to the use of a smart phone application instead of a microplate reader for color intensity quantification (Fig. 1). The plates were made using a CA suspension containing glycerol and calcium carbonate (Fig. 1a). A 3D mold was used to create the microwell structure which was then refined through a series of post fabrication treatments as explained in the methodology section. The plates were made water resistant to prevent absorption of samples through capillary action by spraying them with commercially available water repellant, Scotchgard. Fig. 1b presents the scheme for performance of colorimetric assays in the CA plates and sensing of color intensities using the Smartphone App: Spotxel® Reader.

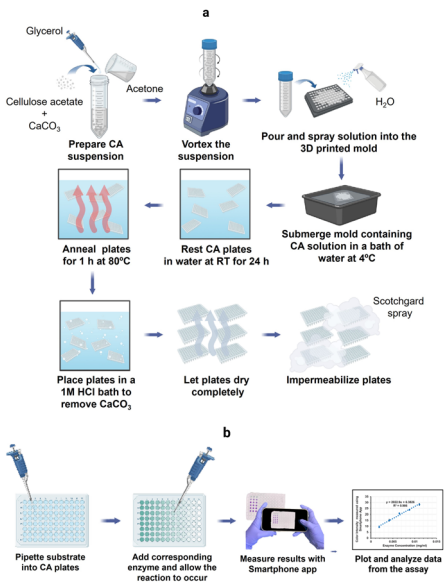


Fig. 1 (a) Scheme for fabrication of CA microwell plate; (b) performance of colorimetric assay in CA microwell plate (created with https://www.biorender.com/).

## 3.1 Fabrication and characterization of CA microwell plates

CA microwell plates were fabricated in 96- and 384-wells formats (Fig. 2a and b). As different processes in laboratory require microwell plates with specific well shapes,[11] we attempted making CA plates with two different shapes of wells: conical and round-bottomed (Fig. 2c–e). Molds for this purpose were designed and printed in a 3D printer (Fig. 2f and g). The volumes of the wells were determined to be 50–185 μL in plates with conical wells (using differently sized wells in the 3D mold) and 70 μL for round-bottom wells. These well volumes are somewhat smaller than those of commercially available PS plates (conical, 300 μL and round bottom, 330 μL).

The CA plates were fabricated using a CA solution in acetone with $CaCO_3$ and glycerol dispersed in it. Glycerol acts as a plasticizer thus reducing the brittleness and fragility of the plates[38] and $CaCO_3$ allows controlled pore formation.[29] While pores are not desirable for the intended application in this study, in the absence of $CaCO_3$, a thin wrinkled film is formed that is relatively fragile and appears very different from the plates being reported in this study. Fabricating the plates in presence of $CaCO_3$ yields a robust self-standing plate and the subsequent removal of $CaCO_3$ using a HCl bath does not affect the structure adversely.

The fabrication of CA plates involved three stages (Fig. 1). In Stage 1 (fabrication) CA/glycerol/$CaCO_3$ dispersion in acetone was poured into the mold in multiple layers (layering technique), resulting in robust and easy-to-handle structures. SEM analysis of the plate at this stage (Fig. 3a) showed a mostly non-porous structure with white spots ($CaCO_3$). Stage 2 (post-fabrication treatments) involved a series of steps. First, the plates were annealed by immersing them in hot water (85 °C for 30 min) which facilitates rearrangement of the membrane structure[31] and formation of pores through the dissolution of some of the calcium carbonate trapped in the plate (Fig. 3b). Annealing also allowed the CA microwell plates to dry flatter without curving, compared to those that were not annealed. This process was followed by treatment with HCl solution to remove the remaining $CaCO_3$ (through its reaction with the acid) and glycerol from the plates.[32,39] FTIR spectra of the plate before and after treatment with HCl bath have been included in Online Resource 1. The spectra confirm the removal of glycerol from the plate after treatment with HCl bath. The HCl bath also removed the $CaCO_3$ from the plate leaving behind a relatively porous structure (Fig. 3c). The shapes of wells, as observed on the rear side of the plate (Fig. 2c–e), were largely uniform. SEM images showed pores of variable sizes distributed throughout the examined surface areas of the plate. The variation in pore size is assumed to be caused by the presence of $CaCO_3$ clusters of different sizes. In Stage 3 (impermeabilization), the plates were spray coated with a commercially available water repellent, *Scotchgard Outdoor Sun & Water Shield Fabric Spray*, to prevent the absorption of aqueous samples by the plate. SEM analysis of the coated CA plates showed a uniform distribution of the

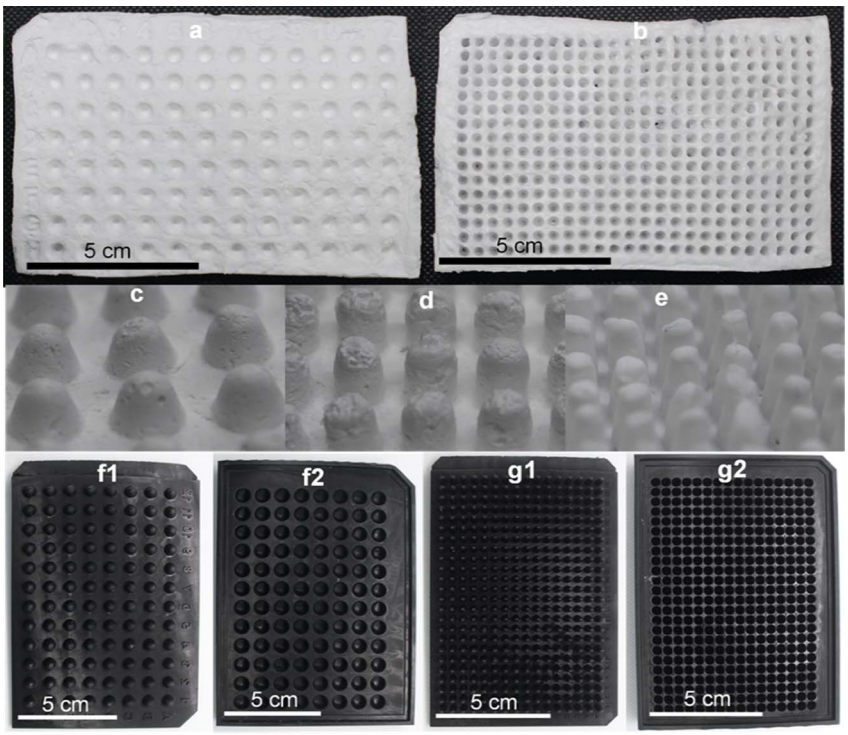


Fig. 2 (a) 96-well CA plate with conical wells; (b) 384-well CA plate with round-bottom wells. Rear side of CA microwell plate demonstrating the different shapes of well: (c) conical wells in 96-well CA plate, 5 mm deep; (d) round-bottom wells in 96-well CA plate, 10 mm deep; (e) round-bottom wells in 384-well CA plate, 10 mm deep. Increasing depth of wells in otherwise similar molds allowed fabrication of CA plates with higher well volumes. 3D printed molds for: (f1–f2) 96-well plate and lid; (g1–g2) 384-well plate and lid.

impermeabilizing agent on the plate surface as pores visible in SEM image of nontreated CA plate appear covered in SEM images of the Scotchgard sprayed membranes (Fig. 3d). A few large crevices are visible on the plate after impermeabilization, which are possibly structural imperfections resulting from the layering technique.

Water absorption experiments on the nontreated and treated plates showed that while a drop of water (10 μL) was absorbed immediately into the non-coated plates, it took 57 ± 1 min in the Scotchgard-treated plates, which is more than the time needed for most colorimetric assays. The coating was found to be effective also with basic and acidic solutions up to concentrations of 0.1 M. Plates that had been exposed to 0.1 M NaOH/HCl showed no alterations to the coating as determined by SEM imaging (Fig. 3d–f). Water absorption experiments on membranes that had been exposed to these solutions showed that water absorption times were similar to those for a plate that had been impermeabilized but not exposed to any of these

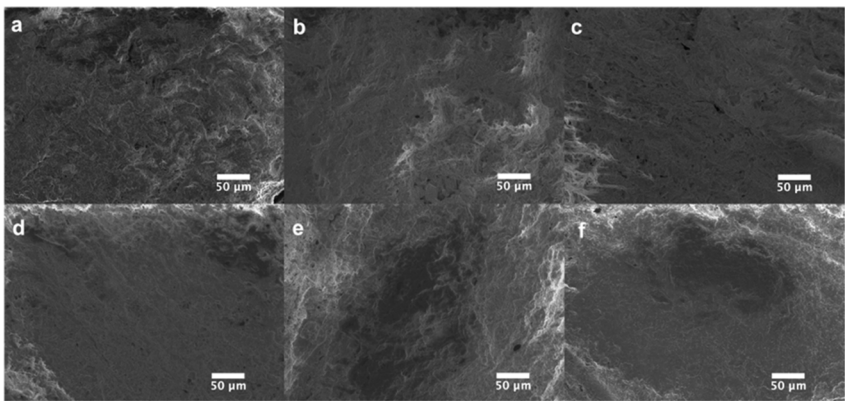


Fig. 3 Scanning Electron Microscope (SEM) images of CA microwell plates at different stages of fabrication. (a) After first stage of fabrication (no post-treatment); (b) after annealing with hot water (1 h at 85 °C); (c) after annealing followed by immersion in HCl bath for $CaCO_3$ removal; (d) final version of the CA microwell plate obtained after annealing treatment, HCl bath, and three coats of Scotchgard. Effect of acid/base on the impermeabilizing layer on the plate: (e) after allowing 10 μL of 0.1 M HCl to be absorbed completely into the well (absorption time: 64 ± 2 min); and (f) after allowing 10 μL of 0.1 M NaOH to be absorbed completely into the well (absorption time: 62 ± 1 min).

solutions. This provided further confirmation of the resistance of the coating to the acidic and basic solutions tested.

### 3.2 Efficacy of CA microwell plates as platforms for colorimetric assays

Three different colorimetric methods were performed in two systems: (i) classic PS 96-well plates using microplate reader for quantification of color intensities, and (ii) CA 96-well plates using the Spotxel® Reader application for smartphones as the color intensity quantifying tool. CA microwell plates holding the assay mixtures are shown in Fig. 4a–c. Row A in Fig. 4a–c represents substrate/buffer blanks in triplicates for each of the three assays. Microwell plate rows B–F contain five different concentrations of the respective analyte in triplicates for each assay. The absorbance/color intensity data was processed to build standard activity plots (Fig. 4d–f) and determine the Limit of Detection (LOD) and Limit of Quantification (LOQ) values for each assay in both systems.

Standard curve for CT activity was generated by monitoring CT catalyzed hydrolysis of the chromogenic substrate SAAPPpNA.[35] This reaction results in the formation of a yellow-colored product, PNA. The quantity of PNA formed was monitored by measuring absorbance at 410 nm, using a UV/Vis microplate reader, in the case of PS microwell plates, and color intensity (using the smartphone app) in case of CA microwell plates. Fig. 4d shows the results obtained when five different dilutions of CT were added to assay mixtures containing identical amounts of SAAPPpNA. All measurements, performed in triplicate, were corrected for background signal by subtracting the blank (buffer + substrate) measurement from them. PNA formation was observed to be directly proportional to the quantity of CT added in both systems tested.

BCA method is a routinely used colorimetric method for protein quantification. It is based on the reduction of $Cu^{2+}$ ions to $Cu^{+}$ by proteins, resulting in a purple-colored complex formation between $Cu^{+}$ ions and the BCA. The protein concentration is directly proportional to intensity of purple color formed which can be quantified by measuring absorbance of the reaction mixture at 562 nm, using a UV/Vis microplate reader, in the case of PS microwell plates, and color intensity (using the smartphone app) in case of CA microwell plates. Fig. 4e shows the standard plots for BCA method in the two systems. Different dilutions of bovine serum albumin (BSA) were allowed to react with same amounts of BCA reagents and resulted in a linear standard plot where the purple-colored complex formation showed a linear increase with an increase in protein concentration in both systems.

The assay used for measuring AP activity is based on hydrolysis of PNPP by AP resulting in the formation of a yellow-colored product PNP. The enzyme activity is directly proportional to the amount of PNP formed, which was quantified by measuring the absorbance of the reaction mixture at 405 nm,

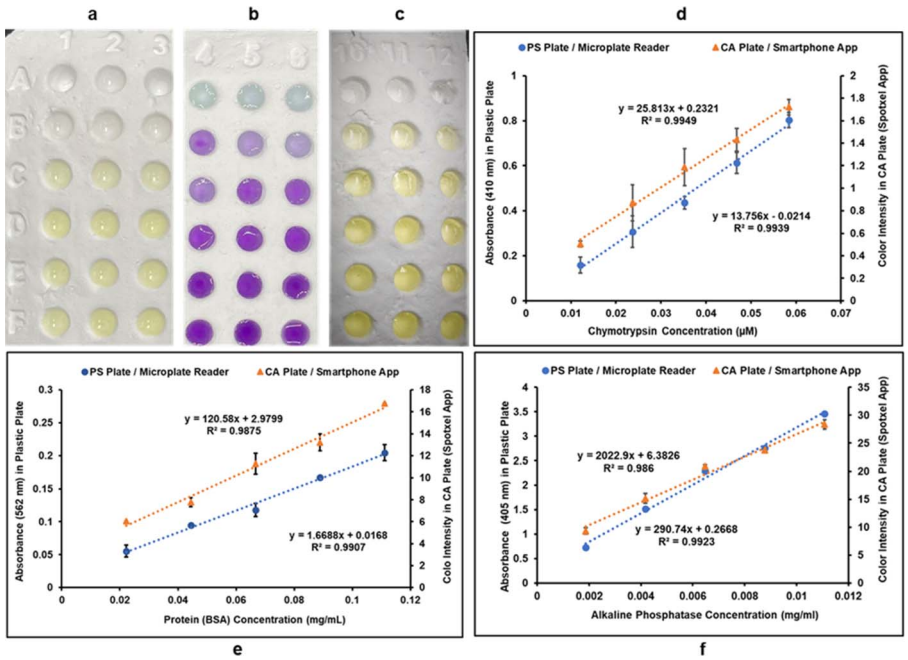


Fig. 4 Colorimetric assays in 96-well CA plates: round-bottom 96-well CA plates were used to perform (a) chymotrypsin assay (hydrolysis of *N*-succinyl-Ala-Ala-Pro-Phe-*p*-nitroanilide); (b) bicinchoninic acid assay (BCA); and (c) alkaline phosphatase assay (hydrolysis of *p*-nitrophenyl phosphate). In (a–c), row A represents substrate/buffer blanks in triplicates for each of the three assays. Rows B–F contain five different concentrations of the respective analyte in triplicates for each assay. Plots (d–f) show quantitative analysis of results obtained for each of the three colorimetric assays (chymotrypsin assay, bicinchoninic acid assay, and alkaline phosphatase assay, respectively) in both PS (○ in blue) and CA microwell plates (Δ in orange). The primary *Y* axis in this figure. (d–f) Represents the absorbance measured for each of the three assays performed in PS plates using a microplate reader (data presented as blue lines); while the secondary *Y* axis represents color intensities measured for each assay in CA plates using the Spotxel Reader application (data presented as orange lines).

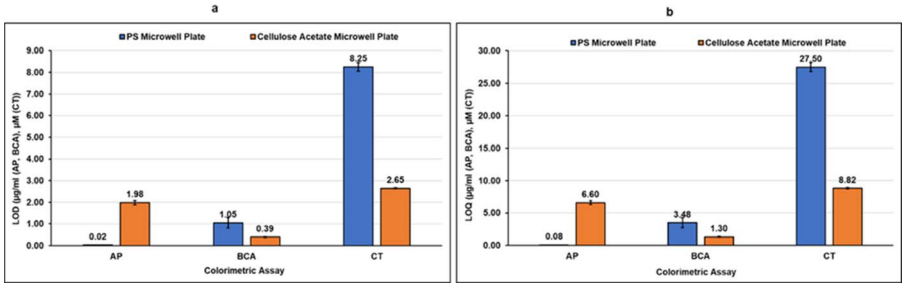


Fig. 5 (a) Limit of Detection (LOD), (b) Limit of Quantification (LOQ) for the three colorimetric assays: alkaline phosphatase (AP) assay, bicinchoninic acid assay (BCA), and chymotrypsin (CT) assay, in both polystyrene and cellulose acetate microwell plates.

using a UV/Vis microplate reader, in the case of PS microwell plates, and color intensity (using the smartphone app) in case of CA microwell plates. Different dilutions of enzyme solution were used in the reaction mixture to generate a standard curve for AP activity. PNP formation was observed to be directly proportional to AP concentration in both systems, as can be observed in Fig. 4f.

As can be observed in Fig. 4d–f from the linear correlation coefficients in each case (Fig. 4d–f), the scale of absorbance is different from the scale of color intensities due to the different reading mechanisms (microplate reader *versus* smartphone app) and thus the *Y*-axis intercepts and slopes are not comparable for the same assay performed in CA plates and PS plates. The linear correlation coefficients ($R^2$), however, are independent of the any differences in scale, and hence can be used to compare the two systems. The linearity of the method using CA plates and Spotxel® Reader yielded accuracy comparable to that obtained using the traditional system based on PS plates and a microplate reader. Limit of Detection (LOD) and Limit of Quantification (LOQ) were also determined for each assay in each of the two systems (Fig. 5), and the values obtained were comparable. This indicates that the CA plates do not affect the sensitivity, precision or accuracy of the assay adversely, and provide as effective a platform as the classic PS plates for colorimetric assays.

Due to the opaque nature of the plate, any minor structural defects in well bottoms (rear side, Fig. 2c–e) do not affect the images for analysis through the smartphone application. This was evidenced by the consistent results obtained from assays performed by different users in plates fabricated by different students and repeated multiple times over the course of one year. An interesting observation was that the opaque white background of these plates allows enhanced observation of samples in the wells thus reducing pipetting errors that occur more frequently in clear transparent plates. CA devices tend to suffer from color uniformity issues, but this limitation was overcome in this study with the Scotchgard treatment. And, while the use of Scotchgard for surface impermeabilization is less than ideal from an environmental standpoint, a single 10 oz cannister can coat at least 37 CA multiwell plates. Additionally, in a separate ongoing study in our laboratory (unpublished yet), we have observed that the Scotchgard coating can be easily removed from the plate by soaking it in a detergent solution and the plate can then be recycled using standard recycling methods for cellulose acetate.

The simplicity of the CA multiwell fabrication process will allow users to make their own plates and customize the fabrication process according to their requirements, for example, with respect to number of wells, and the size, volume, and shape of wells. The fabrication of these plates requires neither sophisticated infrastructure nor skilled labor, as demonstrated by several undergraduate students after a few practice sessions. Also, the CA plates can be modified chemically to manipulate their hydrophobicity/hydrophilicity, and to add functional groups or molecular species that might facilitate specific reactions as we have demonstrated before with commercially available cellulose membranes.[27] Several chemistries that have been developed to derivatize and functionalize cellulose will allow modification of these plates and expand their application along the line of PS plates.[40–44] The use of a smart phone application to measure color intensities also eliminates the need for expensive instruments such as microplate readers.

We have clearly demonstrated the usability of these CA microwell plates for colorimetric assays with high precision and accuracy, which provides viable alternatives to the PS plates in research/diagnostic laboratories, and CA plates could be particularly attractive in academic laboratories. There is great value in students learning to fabricate their own microwell plates, performing assays, and collecting data by simply downloading an app on their smartphones. This exercise shows the power of chemical synthesis to generate macroscopic useful devices and reduces the curricular dependence on microplate readers, which become bottlenecks particularly in large classes. The plates have enormous potential as they can serve as templates for processes ranging from color- and fluorescence-based analytical methods to cell culture and crystallization. During the pandemic it was challenging even in first-world countries to obtain microwell plates, due to supply chain constraints.[45–47] These new plates open environmentally friendly avenues for doing high-throughput assays even under the most challenging research conditions.

## 4 Conclusions

The overarching and ever-increasing dependence of scientific laboratories on single use plastic LabWare has led to their unprecedented contribution to plastic waste worldwide.[3] This

calls for an accelerated drive to develop biodegradable alternatives to such laboratory consumables.[48] In line with this need, we have reported in this manuscript, the fabrication of CA microwell plates as a robust and practical alternative to traditional PS plates. The fabrication process is simple and does not require any advanced skills or instruments besides a mold for plate fabrication which can be printed using 3D printer on-site (if available) or procured from commercial suppliers. A smartphone application was used to quantify the color intensities resulting from the colorimetric assay. The results obtained in CA plates were comparable in accuracy and precision to the measurements performed in commercial PS plates using microplate readers. CA plates, thus, provide not only a biodegradable alternative to PS plates, but also an "instrument-free" analytical tool. This could transform how colorimetric assays are performed in many laboratory settings, and the quantity of plastic waste that is being generated in laboratories all over the world. In the past, we have modified CA discs chemically and demonstrated their feasibility as a template for fluorometric estimations.[49] The CA microwell plates will similarly form excellent platforms for fluorescence-based assays too. CA is highly amenable to chemical modification. The surface of CA microwell plates can easily be modified with sensing molecules of interest thus opening them to a plethora of applications. Further optimization of plate fabrication process with respect to porosity and impermeability to aqueous solutions will allow the plates to be used for applications and processes such as cell culture and crystallization. The ease of customization of CA well dimensions and surface chemistry as per the needs of the end user lends to the promise of CA microwell plates as promising green alternatives to PS microwell plates.

## Author contributions

All authors contributed to the study conception and design. Material preparation and data collection were performed by Gabriela B. Gomez-Dopazo, Renis J. Agosto Nieves, Rolando L. Albarracín Rivera, Daniel Rivera Nazario, and Shaneily M. Colon Morera. Analysis was performed by Vibha Bansal, Gabriela B. Gomez-Dopazo, Rolando L. Albarracín Rivera, Shaneily M. Colon Morera, and Renis J. Agosto Nieves. The first draft of the manuscript was written by Vibha Bansal and all authors commented on previous versions of the manuscript. All authors read and approved the final manuscript.

## Conflicts of interest

There are no conflicts to declare.

## Acknowledgements

This project was supported by the National Science Foundation grant, NSF-DMR-2122102. Support was also received from Instrumentation facilities created through Institutional Development Award (IDeA) from the National Institute of General Medical Sciences of the National Institutes of Health under grant number P20 GM103475. Mr Rolando Albarracin received a research fellowship from NIH-RISE Program at the University of Puerto Rico in Cayey (Grant Number 5R25GM059429-20) to participate in this research. The contents of this manuscript are solely the responsibility of the authors and do not necessarily represent the official view of the NSF or NIH.

## References

1 UNESCO, *UNESCO Science Report: the Race against Time for Smarter Development*, UNESCO, Paris, 2021.
2 *ChemistryViews*, European Chemical Societies Publishing, 2023.
3 J. Alves, F. A. Sargison, H. Stawarz, W. B. Fox, S. G. Huete, A. Hassan, B. McTeir and A. C. Pickering, *Access Microbiol.*, 2020, **3**(3), DOI: **10.1099/acmi.0.000173**.
4 A. Bell, *Guardian*, 2019, **https://www.theguardian.com/environment/2019/nov/10/**.
5 L. Howes, *ACS Cent. Sci.*, 2019, **5**, 1904–1906.
6 M. A. Urbina, A. J. R. Watts and E. E. Reardon, *Nature*, 2015, **528**, 479.
7 W. R. de Araujo and T. R. Paixao, *Paper-based Analytical Devices for Chemical Analysis and Diagnostics*, Elsevier Inc., 2021.
8 G. Ij. Salentijn, M. Grajewski and E. Verpoorte, *Anal. Chem.*, 2018, **90**, 13815–13825.
9 J. Fan, S. Zhang, F. Li, Y. Yang and M. Du, *Cellulose*, 2020, **27**, 9157–9179.
10 A. W. Martinez, S. T. Phillips, M. J. Butte and G. M. Whitesides, *Angew. Chem., Int. Ed.*, 2007, **46**, 1318–1320.
11 D. S. Auld, P. A. Coassin, N. P. Coussens, P. Hensley, C. Klumpp-Thomas, S. Michael, G. S. Sittampalam, O. J. Trask, B. K. Wagner, J. R. Weidner, M. J. Wildey and J. L. Dahlin, in *Assay Guidance Manual*, Eli Lilly & Company and the National Center for Advancing Translational Sciences, Bethesda (MD), 2020.
12 B. T. Ho, T. K. Roberts and S. Lucas, *Crit. Rev. Biotechnol.*, 2018, **38**, 308–320.
13 A. Nilghaz, L. Guan, W. Tan and W. Shen, *ACS Sens.*, 2016, **1**, 1382–1393.
14 S. Nishat, A. T. Jafry, A. W. Martinez and F. R. Awan, *Sens. Actuators, B*, 2021, **336**, 129681.
15 S. Bidmanova, M.-S. Steiner, M. Stepan, K. Vymazalova, M. A. Gruber, A. Duerkop, J. Damborsky, Z. Prokop and O. S. Wolfbeis, *Anal. Chem.*, 2016, **88**, 6044–6049.
16 T. Ozer, C. McMahon and C. S. Henry, *Annual Rev. Anal. Chem.*, 2020, **13**, 85–109.
17 K. E. Boehle, C. S. Carrell, J. Caraway and C. S. Henry, *ACS Sens.*, 2018, **3**, 1299–1307.
18 M. Ornatska, E. Sharpe, D. Andreescu and S. Andreescu, *Anal. Chem.*, 2011, **83**, 4273–4280.
19 A. W. Martinez, S. T. Phillips, E. Carrilho, S. W. Thomas, H. Sindi and G. M. Whitesides, *Anal. Chem.*, 2008, **80**, 3699–3707.
20 E. Noviana, T. Ozer, C. S. Carrell, J. S. Link, C. McMahon, I. Jang and C. S. Henry, *Chem. Rev.*, 2021, **121**, 11835–11885.

21 M. Borah, D. Maheswari and H. S. Dutta, *Microfluid. Nanofluid.*, 2022, **26**, 99.
22 E. Carrilho, S. T. Phillips, S. J. Vella, A. W. Martinez and G. M. Whitesides, *Anal. Chem.*, 2009, **81**, 5990–5998.
23 E. Carrilho, A. W. Martinez and G. M. Whitesides, *Anal. Chem.*, 2009, **81**, 7091–7095.
24 Q. H. Nguyen and M. I. Kim, *TrAC, Trends Anal. Chem.*, 2020, **132**, 116038.
25 K. Yamada, H. Shibata, K. Suzuki and D. Citterio, *Lab Chip*, 2017, **17**, 1206–1249.
26 R. W. Parker, D. J. Wilson and C. R. Mace, *Sci. Rep.*, 2020, **10**, 11284.
27 E. Fasoli, Y. R. Reyes, O. M. Guzman, A. Rosado, V. R. Cruz, A. Borges, E. Martinez and V. Bansal, *J. Chromatogr. B*, 2013, **930**, 13–21.
28 C. J. Ortiz-Hernandez, A. N. Santiago-Ruiz, A. J. Torres-Rosado, J. Jiménez-Gonzalez, S. B. Yeldell, R. Oyola, I. J. Dmochowski, J. Sotero-Esteva, V. Bansal and E. Fasoli, *Anal. Bioanal. Chem.*, 2019, **411**, 1549–1559.
29 A. Kaiser, W. J. Stark and R. N. Grass, *J. Chem. Educ.*, 2017, **94**, 483–487.
30 A. F. de Faria, A. C. M. de Moraes, P. F. Andrade, D. S. da Silva, M. do Carmo Gonçalves and O. L. Alves, *Cellulose*, 2017, **24**, 781–796.
31 T. P. N. Nguyen, E.-T. Yun, I.-C. Kim and Y.-N. Kwon, *J. Membr. Sci.*, 2013, **433**, 49–59.
32 Z. Mohammed Redha, Q. Bu-Ali, Y. A. Saeed and A. M. Ali, *Arabian J. Sci. Eng.*, 2021, **46**, 6593–6607.
33 P. K. Smith, R. I. Krohn, G. T. Hermanson, A. K. Mallia, F. H. Gartner, M. D. Provenzano, E. K. Fujimoto, N. M. Goeke, B. J. Olson and D. C. Klenk, *Anal. Biochem.*, 1985, **150**, 76–85.
34 X. Chen, J. Chen, H.-Y. Zhang, F.-B. Wang, F.-F. Wang, X.-H. Ji and Z.-K. He, *Chin. J. Anal. Chem.*, 2016, **44**, 591–596.
35 M. W. Jaworek and R. Winter, *ChemSystemsChem*, 2020, **3**(2), e2000029.
36 L. Han, H. Zhang, D. Chen and F. Li, *Adv. Funct. Mater.*, 2018, **28**, 1800018.
37 R. Zhang, N. Lu, J. Zhang, R. Yan, J. Li, L. Wang, N. Wang, M. Lv and M. Zhang, *Biosens. Bioelectron.*, 2020, **150**, 111881.
38 J. Tarique, S. M. Sapuan and A. Khalina, *Sci. Rep.*, 2021, **11**, 13900.
39 S. C. Teixeira, R. R. A. Silva, T. V. De Oliveira, P. C. Stringheta, M. R. M. R. Pinto and N. D. F. F. Soares, *Food Biosci.*, 2021, **42**, 101202.
40 M. Isik, H. Sardon and D. Mecerreyes, *Int. J. Mol. Sci.*, 2014, **15**, 11922–11940.
41 S. Cichosz and A. Masek, *Polymers*, 2019, **11**, 1174.
42 W. Ge, J. Shuai, Y. Wang, Y. Zhou and X. Wang, *Polym. Chem.*, 2022, **13**, 359–372.
43 J. Zhang, Y. Qi, Y. Shen and H. Li, *Mater. Sci.*, 2022, **28**, 60–67.
44 M. H. Hussain, U. M. Zaki, N. F. A. Bakar, H. L. Tan, N. A. Rahman, A. Azizan, N. Adrus, M. H. Haron, L. K. Teh and M. S. Osman, in *Regenerated Cellulose and Composites*, ed. M. Shabbir, Springer Nature Singapore, Singapore, 2023, pp. 79–104.
45 Global Data Healthcare, *Supply shortages negatively impacting not only Covid-19 testing*, **https://www.medicaldevice-network.com/comment/supply-shortages-covid-19-testing**, accessed May 6, 2023.
46 D. Stoyanova, *Cambridge labs face supply shortages and delays*, **https://www.varsity.co.uk/news/21103**, accessed May 6, 2023.
47 K. Zimmer, *Labs worldwide still struggling amid broken supply chains*, **https://www.the-scientist.com/news-opinion/labs-worldwide-still-struggling-amid-broken-supply-chains-68787**, accessed February 11, 2023.
48 Eppendorf, *Science-friendly, planet-friendly: Pipette tips go green via bio-based products*, **https://www.science.org/content/resource/science-friendly-planet-friendly-pipette-tips-go-green-bio-based-products?utm_medium=email&utm_source=publishing-sfmc&utm_campaign=custompubs2023&utm_content=eppendorf&utm_id=recy5o10lg3af4LqP&et_rid=40184802&et_cid=4961383**, accessed November 1, 2023.
49 C. J. Ortiz-Hernandez, A. N. Santiago-Ruiz, A. J. Torres-Rosado, J. Jiménez-Gonzalez, S. B. Yeldell, R. Oyola, I. J. Dmochowski, J. Sotero-Esteva, V. Bansal and E. Fasoli, *Anal. Bioanal. Chem.*, 2019, **411**, 1549–1559.